Heliyon

*Received:*
9 October 2017
*Revised:*
23 January 2018
*Accepted:*
27 April 2018

Cite as: Justin B. Davis, Valerie Calvert, Steven Roberts, Sabrina Bracero, Emanuel Petricoin, Robin Couch. Induction of nerve growth factor by phorbol 12-myristate 13-acetate is dependent upon the mitogen activated protein kinase pathway. Heliyon 4 (2018) e00617. doi: 10.1016/j.heliyon.2018.e00617

# Induction of nerve growth factor by phorbol 12-myristate 13-acetate is dependent upon the mitogen activated protein kinase pathway

**Justin B. Davis*, Valerie Calvert, Steven Roberts, Sabrina Bracero, Emanuel Petricoin, Robin Couch**

*George Mason University, USA*

* Corresponding author.
E-mail address: jdavis17@gmu.edu (J.B. Davis).

## Abstract

Several small molecules have been identified that induce glial cells to synthesize and secrete nerve growth factor (NGF), a critical neurotrophin that supports neuronal growth and survival, and as such show promise in the development of drugs for the chemoprevention of Alzheimer's disease. To map the signal transduction cascade leading to NGF synthesis and secretion, cultured human glial cells were stimulated by phorbol 12-myristate 13-acetate (PMA), an agonist of Protein Kinase C. Changes in intracellular protein phosphorylation states were evaluated by reverse phase protein microarrays (RPPA), selectively screening over 130 protein endpoints. Of these, 55 proteins showed statistically significant changes in phosphorylation state due to cellular exposure to PMA. A critical signal transduction pathway was identified, and subsequent validation by ELISA and qPCR revealed that the signaling proteins Raf, MEK, ERK, and the signal transduction factor CREB are all essential to the upregulation of NGF gene expression by PMA. Additionally, members of the RSK family of kinases appear to be involved in glial secretion (exocytosis) of the NGF protein. Furthermore, through RPPA, the effects of PMA on apoptosis signaling events and cell

https://doi.org/10.1016/j.heliyon.2018.e00617

proliferation were differentiated from the pathway to NGF upregulation. Overall, this study reveals potential protein targets for the rational design of Alzheimer's therapeutics.

Keywords: Molecular biology, Neuroscience, Biochemistry, Cell biology

## 1. Introduction

Alzheimer's Disease (AD), the most prevalent cause of dementia, affects over 46 million people worldwide [1]. The underlying etiology of the disease remains unknown, so efforts to combat AD generally focus on targeting the known pathology. This neurodegenerative disease is typically characterized by the accumulation of beta-amyloid [2, 3, 4], hyperphosphorylation of tau protein and development of neurofibrillary tangles [2, 5, 6], and the loss of brain matter, particularly the loss of basal forebrain cholinergic neurons (BFCN) [7, 8, 9]. The BFCN region is one of the earliest and most severely affected regions of the AD brain, and the loss of these neurons is a critical component of the cognitive decline observed in disease progression [10, 11, 12]. Approved therapeutics for AD generally target the process of neurotransmitter signaling, but do not substantially slow nor reverse the course of the disease [2]. Clinical trials with therapies designed to lower the amyloid burden have also shown little success in delaying the progression of the disease [13]. In contrast, one promising avenue for retarding AD lies in preventing degeneration of the BFCN via the administration of nerve growth factor (NGF).

NGF and its high affinity receptor, TrkA, are well expressed in the basal forebrain of healthy individuals [14]. Binding of mature NGF to TrkA initiates a signaling cascade that results in axonal guidance, neurite outgrowth, upregulation of cell-survival pathways, and suppression of caspase activity and apoptosis [15, 16, 17, 18, 19]. An imbalance in NGF levels and TrkA expression are observed in AD [11, 14], and thus, much interest exists in NGF restorative therapies. Due to its size and polarity, NGF is unable to freely penetrate the blood brain barrier [20, 21]. Hence, preclinical and clinical investigations of NGF have utilized receptor mediated transport across the blood brain barrier [20, 22], grafting of NGF expressing cells [23], or stereotactic delivery of viral expression systems [12, 24], among other invasive techniques. Overall, the results have been encouraging, with NGF-treated subjects exhibiting a restoration of brain matter and gain in cognitive function relative to untreated controls [12]. Long-term supplementation of NGF appears to be well tolerated and clinical trials in persons with AD suggest reduction in the rate of AD-induced cognitive decline [12]. However, the cost and invasiveness of these procedures is restrictive, lending them to be poorly suited to treat the large, widespread population that suffers from AD. One practical alternative may rest in the form of an oral or inhalable administered therapeutic, capable of traversing the blood brain barrier and inducing glial cell secretion of NGF *in situ*.


https://doi.org/10.1016/j.heliyon.2018.e00617

Phorbol 12-myristate 13-acetate (PMA) is a known agonist of protein kinase C [25] and a potent inducer of NGF gene expression and secretion [21]. However, phorbol esters such as PMA also affect proliferative and cell survival pathways within the cell and have long been recognized as powerful tumor promoters [26, 27, 28] and apoptosis inducers [29, 30, 31, 32, 33, 34], depending upon the phorbol ester concentration and the state of the cell and its microenvironment. Hence, the clinical use of PMA (and other phorbol ester analogs) as an inducer of NGF is undesirable. Accordingly, distinguishing the mechanism by which PMA stimulates NGF expression and secretion from its tumor promoting or apoptotic activity might reveal protein targets for the rational development of nontoxic NGF-inducing therapeutics. In the research described herein, we aimed to deconvolute the therapeutic effects of PMA as an inducer of NGF from its activity as a tumor promoter and toxic agent. To accomplish this, we used cultured human glioblastoma cells and reverse phase protein microarrays to identify key proteins and signaling pathways activated and suppressed in response to PMA. Our array results revealed the activation of multiple signaling pathways relating to tumorigenesis, apoptosis, and inflammation, as well as the activation of central regulatory pathways such as the MAPK/ERK cascade. Using a combination of NGF ELISA, quantitative PCR (qPCR), cell viability assays, and specific protein agonists and antagonists, we were able to define and validate the signal transduction cascade underlying the PMA upregulation of NGF. Our results reveal that PMA induction of NGF gene expression and secretion is dependent upon the activation of PKC and the activity of MEK, ERK, and p90RSK.

## 2. Results and discussion

### 2.1. $EC_{50}$ of PMA-Induced NGF secretion

An aim of our investigation is to deconvolute the signal transduction pathways underlying the therapeutic effects of PMA as an inducer of NGF from those underlying its more undesirable effects. To map the signal transduction pathway associated with PMA-induced NGF induction, we first determined the half-maximal activity of PMA, so as to minimize off-targeting of PMA (binding to lower affinity protein targets) while maintaining substantial NGF induction. Cultured human glial cells were exposed for 12 hours to various concentrations of PMA and then NGF titers were experimentally determined by NGF ELISA. A sigmoidal dose response was achieved and the $EC_{50}$ was determined to be 6.6 nM (Fig. 1). For convenience, 10 nM PMA was used for mapping signal transduction via reverse phase protein microarrays.

### 2.2. The transcription factor CREB

Cyclic AMP response element-binding protein (CREB) has been previously implicated in the expression of the NGF gene [35, 36]. To test for its involvement in PMA


https://doi.org/10.1016/j.heliyon.2018.e00617

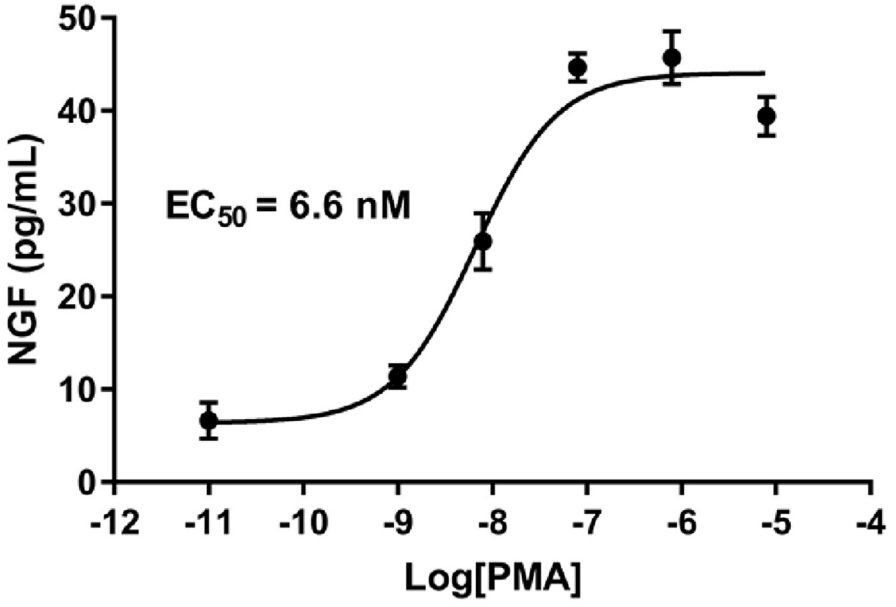


**Fig. 1.** The PMA dose response. Cultured human glial cells (T98G) were incubated for 12 hours with the indicated concentration of PMA and then secreted NGF titers were determined using an NGF-specific ELISA. All assays were performed in at least triplicate. Non-linear regression fitting indicates the half-maximal activity of PMA occurs at 6.6 nM ($R^2 = 0.95$). Notably, a suppression of NGF titer is observed at an elevated PMA concentration (10 μM), likely reflective of phorbol-ester cytotoxicity [32, 33].

upregulation of NGF, we assayed NGF gene expression and protein secretion from T98G cells exposed to PMA, both with and without compound 217505, a commercially available inhibitor of CREB. As shown in Fig. 2A, at 1 μM concentration, compound 217505 has no deleterious effect on the viability of the cultured glial cells. Additionally, 1 μM 217505 has no significant effect on the amount of NGF that is secreted by the cell culture in response to PMA within four hours (Fig. 2B). This four hour period is likely insufficient to complete the transcription, translation, and exocytosis necessary to contribute detectable increases in NGF titers. The compound 217505 does, however, significantly reduce the abundance of transcript associated with PMA upregulation of NGF gene expression (Fig. 2C), confirming the involvement of CREB in PMA induction of NGF. Detectable increases in NGF secretion within four hours is likely a manifestation of PMA induced exocytosis of NGF already stored within cells. Thus, we aim to determine the mechanism by which PMA induces both *de novo* synthesis of NGF as well as exocytosis of the protein.

## 2.3. Reverse phase protein microarrays (RPPA)

Having established the involvement of CREB in PMA induced upregulation of NGF from cultured human glial cells, we next sought to map the signal transduction


https://doi.org/10.1016/j.heliyon.2018.e00617

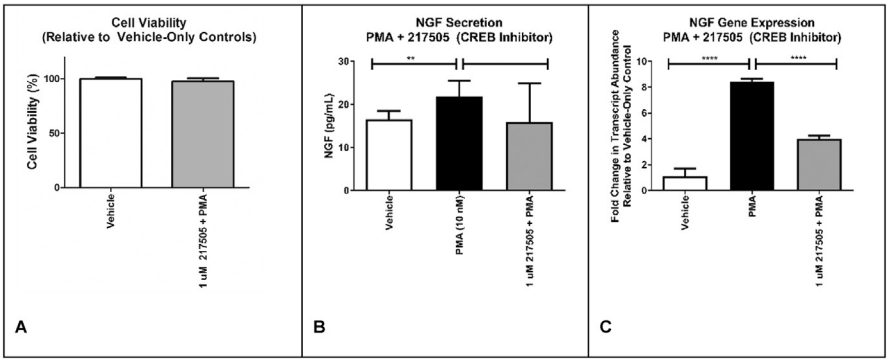


**Fig. 2.** Effects of CREB Inhibitor 217505 on PMA induction of NGF. A) An alamar blue based colorimetric assay was used to determine the viability of cultured human glial cells exposed to vehicle (DMSO) or 10 nM PMA coupled with 1 μM of 217505, as indicated. Percent viability is relative to the culture exposed to vehicle alone. CREB inhibitor 217505 has no effect on glial cell viability, either alone (not shown) or in combination with 10 nM PMA. B) Conditioned media obtained from human glial cell cultures exposed to either vehicle (DMSO), 10 nM PMA, or 10 nM PMA+1 μM 217505 were assayed for NGF content using an NGF-specific ELISA. The glial cells were preincubated with 217505 for 20 mins, then PMA was added and NGF titers were determined after a 4 hr incubation. 217505 has no significant effect on PMA-induced glial cell NGF secretion within four hours. C) Quantitative PCR assessment of NGF transcript in human glial cell cultures treated with vehicle (DMSO), 10 nM PMA, or 10 nM PMA coupled with 1 μM of 217505, as indicated. The cells were treated as described in B). 217505 significantly reduces PMA-induced NGF gene expression ($n = 6$). As a side note, 217505 is insoluble in media at concentrations above 1 μM. All graphs are expressed as Mean + SD.

cascade from PKC through to CREB. RPPA-based pathway mapping was used to quantify the changes in phosphorylation state of 135 different target proteins (Table 1). These analytes were specifically chosen as they include signaling proteins and transcription factors known to regulate cell metabolism, cell proliferation, cell survival, and exocytosis. Human T98G glial cells were cultured to confluence in six-well plates, then the cultures were exposed to either PMA or vehicle (DMSO) for either a 2 minute, 15 minute, 60 minute, or 240 minute duration. Following exposure, the cells were lysed and examined via RPPA. All assays were performed with 6 replicates. In a manner described in detail previously [36, 37, 38, 39], several proteins were identified by RPPA to demonstrate a statistically significant ($p < 0.05$) change in phosphorylation status with exposure to PMA. More specifically, of the 135 analyzed endpoints, 55 proteins showed a statistically significant change due to exposure to 10 nM PMA. As detailed below, the activities of proteins and pathways responsible for regulating apoptosis (Table 2), as well as proteins known to stimulate cell proliferation (Table 3), were clearly altered by PMA. Also detailed below, examination of successive incubation durations allowed us to identify sequential activation along known signal transduction pathways, ultimately highlighting the proteins of the mitogen activated protein kinase (MAPK) pathway (Table 4) as central to the PMA upregulation of NGF.


https://doi.org/10.1016/j.heliyon.2018.e00617

**Table 1.** Antibodies evaluated by reverse phase protein microarray.

| | | |
|---|---|---|
| ATG12 | pc-Abl T735 | pMst1/2 T183/180 |
| Bax | pc-Abl Y245 | pmTOR S2448 |
| Bcl-xL | pCatenin B S33/37/T41 | pNFkB S536 |
| Beclin 1 | pc-Kit Y719 | pNPM T199 |
| Cleaved Caspase-3 D175 | pc-PLA2 S505 | pp27 T187 |
| Cleaved Caspase-6 D162 | pc-Raf S338 | pp38 MAPK T180/Y182 |
| Cleaved Caspase-7 D198 | pCREB S133 | pp53 S15 |
| Cleaved Caspase-9 D330 | pCrkII Y221 | pp70 S6 Kinase S371 |
| Cleaved PARP D214 | pCrkL Y207 | pp70 S6 Kinase T389 |
| c-Met | pCyclin D1 T286 | pp70 S6 Kinase T412 |
| c-Myc | pEGFR Y1068 | pp90RSK S380 |
| c-Src | pEGFR Y1148 | pPAK1/2 S199/204/S192/197 |
| Cyclin A | pEGFR Y1173 | pPDGF Receptor B Y716 |
| Cyclin B1 | peIF2a S51 | pPDGF Receptor B Y751 |
| E-Cadherin | peIF4E S209 | pPKCa S657 |
| EGFR | peIF4G S1108 | pPKCzeta/lambda T410/403 |
| ErbB2 | pElk-1 S383 | pPLCgamma1 Y783 |
| ErbB4 | peNOS S113 | pPLK1 T210 |
| HIF-1a | peNOS/NOS III S116 | pPRAS40 T246 |
| Histone H3, Di-Methyl Lys27 | pErbB2 Y1248 | pPRK1/2 T774/816 |
| Histone H3, Pan-Methyl Lys9 | pErbB2 Y877 | pPTEN S380 |
| IL-6 | pErbB3 Y1289 | pPyk2 Y402 |
| LC3B | pERK T202/Y204 | pRaf S259 |
| NUMB | pEtk Y40 | pRas-GRF1 S916 |
| p4E-BP1 70 | pFADD S194 | pRb S780 |
| p4E-BP1 S65 | pFAK Y576/577 | pRet Y905 |
| p4E-BP1 T37/46 | pFKHR S256 | pRSK3 T356/S360 |
| p53 | pFKHR/FKHRL1 T24/32 | pS6 Ribosomal Protein S235/236 |
| pAcetyl-CoA Carboxylase S79 | pFRS2a Y436 | pS6 Ribosomal Protein S240/244 |
| pAdducin S662 | pGab1 Y627 | pSAPK/JNK T183/Y185 |
| pAKT S473 | pGSK-3a/B S21/9 | pSGK1 S78 |
| pAKT T308 | pHistone H3 S10 | pShc Y317 |
| pALK Y1586 | pHSP27 S82 | pSmad1/5/8 S463/S465/S467 |
| pAMPKa T172 | pHSP90a T5/7 | pSmad2 S465/467 |
| pAMPKa1 S485 | pIGF-1R/IR Y1131/1146 | pSrc Family Y416 |
| pAMPKB1 S108 | pIGF-1R/IR Y1135/36/Y150/51 | pSrc Y527 |
| pArrestin1B S412 | pIkBa S32/36 | pStat1 Y701 |
| pATF-2 T71 | pIRS-1 S612 | pStat3 S727 |
| pATP-Citrate Lyase S454 | pJak1 Y1022/1023 | pStat3 Y705 |

(*continued on next page*)


https://doi.org/10.1016/j.heliyon.2018.e00617

**Table 1.** (*Continued*)

| | | |
|---|---|---|
| pBAD S112 | pJak2 Y1007 | pStat5 Y694 |
| pBAD S136 | pLKB1 S428 | PTEN |
| pBAD S155 | pMDM2 S166 | pTyk2 Y1054/1055 |
| pBcl-2 S70 | pMEK1/2 S217/221 | Survivin |
| pBcr Yb177 | pMet Y1234/1235 | pMst1/2 T183/180 |
| pB-Raf S445 | pMSK1 S360 | pmTOR S2448 |

Lysates from PMA treated and vehicle-treated T98G glial cells (n = 6) were evaluated to quantify the abundance of proteins specific to the antibodies listed.

## 2.4. PMA regulation of apoptosis

As noted above, the protein microarrays demonstrate the effect of PMA signaling on key regulators of apoptosis (Table 2). Specifically, we observed PMA-induced alterations in the abundance and phosphorylation state of intrinsic (mitochondrial mediated) apoptotic signaling proteins, most notably, the Bcl-caspase axis. The Bcl-2 protein family consists of both anti-apoptotic and pro-apoptotic proteins. Anti-apoptotic members of the Bcl-2 family inhibit activation of caspase-9 and p53 mediated apoptosis [40]. Pro-apoptotic members of this protein family, such as Bad and Bax, promote activation of the caspase cascade through binding inhibition of the anti-apoptotic members (Bad) or stimulating cytochrome c mediated apoptosis directly (Bax) [40, 41, 42]. When stimulated by pro-apoptotic Bad and Bax, cytochrome c is released from the mitochondria and induces apoptosome formation [42, 43, 44]. Apoptosome formation generates an active form of caspase 9 which

**Table 2.** Statistically significant changes in abundance of cell death directing proteins.

| **Cell death pathways** | **P-value by exposure duration (min)** | | | |
|---|---|---|---|---|
| **Protein endpoint** | **2** | **15** | **60** | **240** |
| pBAD S112 | | 0.00801 ↑ | 0.00032 ↑ | |
| pBAD S136 | | | 0.02653 ↑ | |
| pBAD S155 | | | 0.03500 ↑ | |
| Bax | | 0.01904 ↓ | | |
| Cleaved Caspase-7 D198 | 0.03378 ↑ | | 0.02972 ↓ | |
| pHSP27 S82 | | 0.0251 ↑ | 0.00126 ↑ | 0.00873 ↑ |
| pMst 1/2 T183/180 | | 0.01007 ↑ | 0.02292 ↑ | |
| Cleaved PARP D214 | 0.04417 ↑ | 0.01665 ↑ | | |
| Survivin | | | 0.04331 ↑ | |

A two-tailed unpaired heteroscedastic t-test was performed to determine whether PMA caused significant change ($p < 0.05$) in the abundance of proteins and phosphoproteins implicated in mediating cell death. Arrows indicate increases or decreases in endpoint abundance.


https://doi.org/10.1016/j.heliyon.2018.e00617

**Table 3.** Statistically significant changes in abundance of proteins involved in cell division.

| Cell Proliferation/Carcinogenic proteins | P-value by exposure duration (min) | | | |
|---|---|---|---|---|
| **Protein endpoint** | **2** | **15** | **60** | **240** |
| pc-Abl | | 0.00286 ↑ | 0.00114 ↑ | |
| pMDM2 S166 | | | 0.00970 ↑ | |
| pMetY1234/1235 | | | 0.03248 ↑ | |
| NUMB | | | 0.00356 ↑ | |
| pPLK1 T210 | | | 0.04029 ↑ | |
| p53 | | | 0.00397 ↑ | |

A two-tailed unpaired heteroscedastic t-test was performed to determine whether PMA caused statistically significant change ($p < 0.05$) in the abundance of proteins and phosphoproteins related to cell proliferation and/or implicated in carcinogenesis. Arrows indicate increases or decreases in endpoint abundance.

can then cleave and activate effector caspases -3 and -7 to promote apoptosis [45] (Fig. 3).

In our results, Bax protein is deactivated by dephosphorylation within 15 minutes of the introduction of 10 nM PMA, suggesting suppression of apoptosis. Downregulation of apoptotic signaling is also evident in the increased abundance of phosphorylated Bad (at S112, S136, and S155). These posttranslational modifications prohibit dimerization of Bad with Bcl-$X_L$ or Bcl-2, preventing downstream signaling of apoptosis [41, 46, 47]. S112 phosphorylation is believed to be a direct result of

**Table 4.** Statistically significant changes in abundance of phosphorylated MAPK signaling proteins.

| MAPK/ERK signal transduction | P-value by exposure duration (min) | | | |
|---|---|---|---|---|
| **Protein endpoint** | **2** | **15** | **60** | **240** |
| pCREB S133 | | 0.02058 ↑ | 0.00062 ↑ | |
| pElk-1 S383 | | 0.00146 ↑ | 0.00701 ↑ | |
| pERK T202/Y204 | | 0.00002 ↑ | 0.00059 ↑ | |
| pMEK 1/2 S217/221 | | 0.03810 ↑ | 0.01037 ↑ | |
| pMSK1 S360 | | 0.00035 ↑ | | |
| pPKCa S657 | | 0.00619 ↓ | 0.03333 ↓ | 0.01591 ↓ |
| pB-Raf S445 | 0.00587 ↑ | 0.00993 ↑ | 0.03395 ↑ | |
| pc-Raf S338 | | 0.00569 ↑ | 0.02553 ↑ | 0.01858 ↑ |
| pp90RSK S380 | 0.01847 ↑ | 0.00530 ↑ | 0.02397 ↑ | |
| pRSK3 T356/S360 | | | 0.00977 ↑ | 0.01321 ↑ |

Two-tailed unpaired heteroscedastic t-tests were performed to determine if PMA caused statistically significant change ($p < 0.05$) in the abundance of phosphorylated MAPK signaling proteins. Arrows indicate increases or decreases in endpoint abundance.


https://doi.org/10.1016/j.heliyon.2018.e00617

Ras and Raf kinase activity [46], and S155 phosphorylation is claimed to be a target of RSK1 kinase activity [41]. These connections are evident within our dataset (Table 4) and reveal a clear link between PMA induction of the MAPK pathway and suppression of Bcl-family apoptotic signaling in T98G cells.

With regards to the caspases, we observed no statistically significant change in the abundance of cleaved caspases-3, -6, or -9. Cleavage of caspase-9, and subsequently caspase-3, is performed by the apoptosome. Apoptosome formation and caspase cleavage is inhibited by Hsp27 [48], and antagonism is enhanced by Hsp27 phosphorylation at S82 [49, 50]. We observed a statistically significant increase in Hsp27 phosphoS82 abundance after 15 minutes, 60 minutes, and 240 minutes of 10 nM PMA exposure, suggesting that PMA suppresses caspase mediated apoptosis throughout this exposure duration. Survivin, a member of the inhibitor of apoptosis family of proteins, inhibits the activities of caspases -3 and -7, likely through inhibition of caspase-9 [51]. A statistically significant increase in Survivin abundance was observed after 60 minutes of PMA exposure, further supporting PMA suppression of apoptosis. We did, however, record a significant change in the abundance of cleaved caspase-7 following 2-minute exposure to PMA. This phenomenon was diminished by the 60-minute time point, suggesting that prolonged exposure to PMA alleviates this effect through activation of the pro-survival signaling mechanisms discussed above.

Despite evidence of apoptosis suppression, we still observed several downstream indicators of caspase activity. PolyADP ribose polymerase (PARP), commonly used as a marker of caspase-mediated apoptosis, is a substrate for caspase and calpain protease families [52, 53]. An increase in cleaved PARP was detected 2 minutes and 15 minutes following exposure to 10 nM PMA. This observation may be attributed to the brief increase in cleaved caspase-7 (described above), which is a known PARP-cleaving protease, or it may be a result of a signaling mechanism not analyzed within our study. A second indicator of apoptosis, phosphorylated Mst, was also significantly upregulated in T98G cells treated with PMA. Mst becomes a better substrate for phosphorylation following cleavage by caspase-3, and thus, the presence of the phosphorylated form is usually associated with caspase activity and apoptosis [54]. These downstream indicators of apoptosis suggest that statistically insignificant changes in caspase activity may amplify into tangible effects on caspase targets or that alternative protease networks are active.

To determine whether the net effects of PMA on apoptotic signaling generate any measurable effects on cell viability, we performed a resazurin based cell viability assay evaluating the toxicity of 10 nM and 100 nM PMA after 4-hour exposure (Fig. 4A). The results indicate a mild, but statistically significant effect on cell viability that increases with PMA concentration. The findings agree with the presence of the downstream caspase markers detected by RPPA analysis, and suggest


https://doi.org/10.1016/j.heliyon.2018.e00617

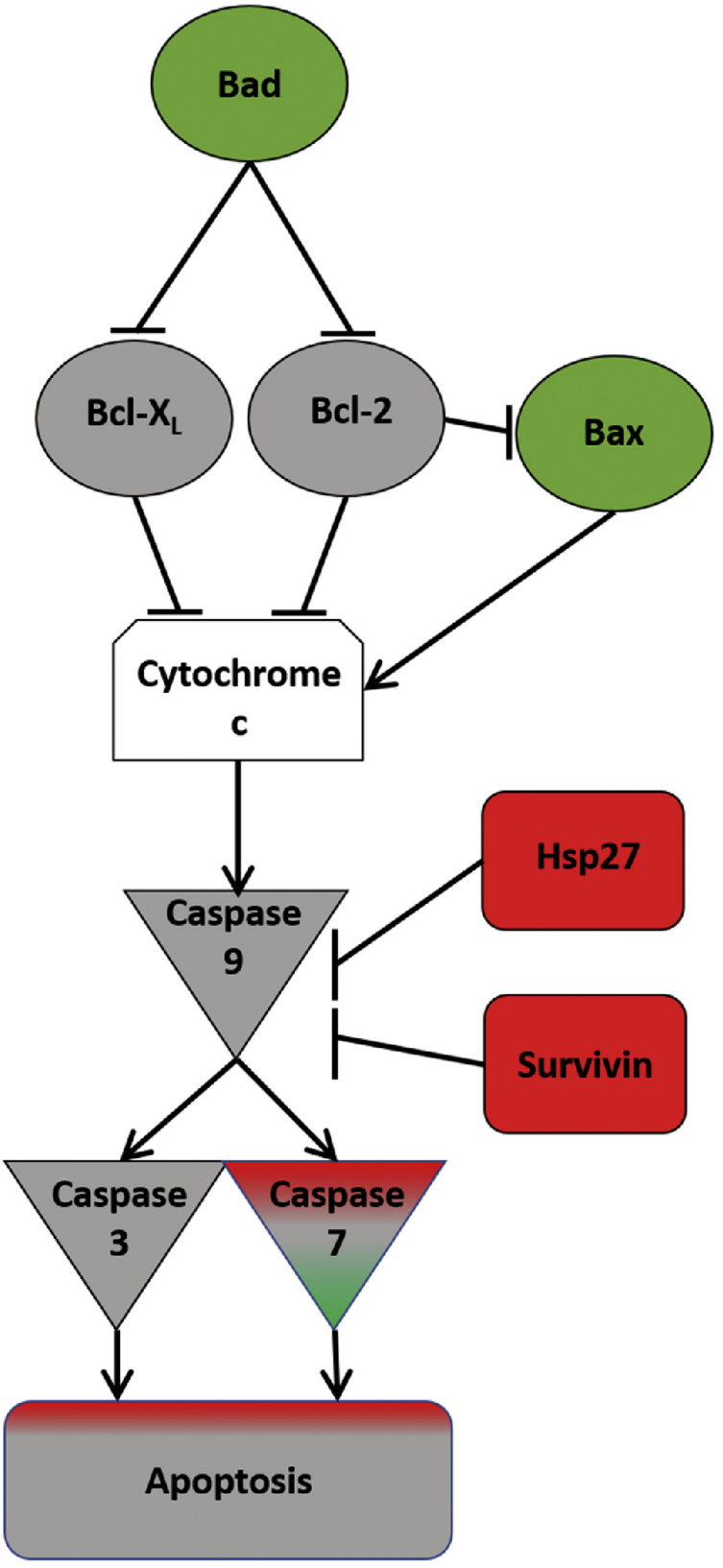



https://doi.org/10.1016/j.heliyon.2018.e00617

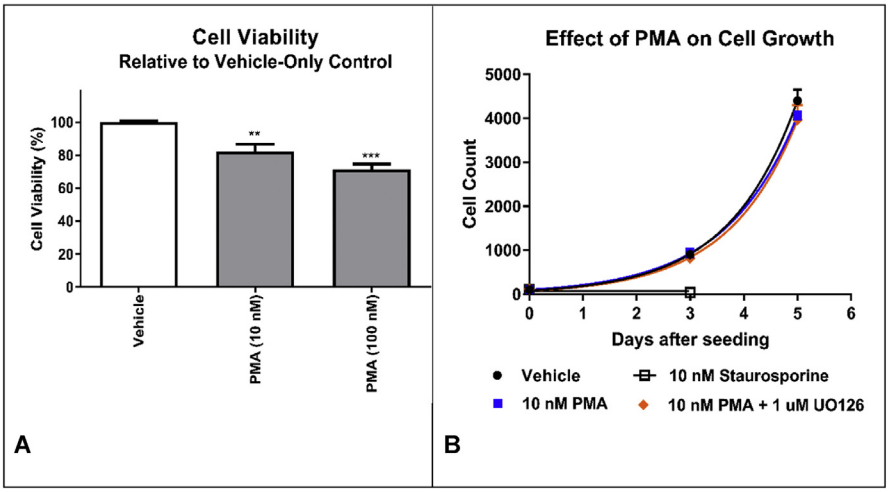


**Fig. 4.** Effects of PMA and MEK inhibitor on cell viability and proliferation. A) T98G cells were treated with PMA or vehicle alone for four hours. After four hours, cell viability was measured by resazurin assay. PMA 10 nM exhibits a mild, but statistically significant ($p < 0.01$, $n = 6$) effect on cell viability at 20% confluence. Cell viability is further reduced at higher concentrations of PMA ($p < 0.001$, $n = 6$). B) T98G cells were seeded at 20% confluence and treated with 10 nM PMA in the presence and absence of MEK inhibitor UO126 (1 μM) 24 hours after seeding and again 72 hours after seeding. Cells were counted at initial seeding (Day 0), after 3 days, and after 5 days. No statistical significance ($n = 6$ replicates) is observed when comparing the doubling times of vehicle. Control cells (22.6 hours, $R^2$ value of 0.9943), 10 nM PMA treated cells (23.3 hours, $R^2$ value of 0.999), and 10 nM PMA treated cells supplemented with UO126 (24.7 hours, $R^2$ value of 0.987). A known toxic agent, staurosporine, was used at 10 nM concentration as a positive control to illustrate the effects of significant toxicity on T98G cells. All graphs are expressed as Mean + SD.

that PMA-induced toxicity happens immediately following exposure. To determine whether PMA has long-term effects on cell viability, we evaluated 5-day cell growth in the presence of 10 nM PMA (Fig. 4B). A MEK inhibitor was also included in the study to confirm that the MAPK signaling pathway, another major signaling cascade significantly activated by PMA exposure, was not regulating alterations to cell viability and proliferation. T98G cells were seeded at 20% confluence and treated with 10 nM PMA in the presence and absence of MEK inhibitor UO126 (1 μM) after 24 hours and 72 hours. Evaluating at day 3 and again at day 5, we found no statistically significant decrease in treated cell proliferation, compared to untreated controls. Thus, these results support our observations that PMA inhibits the intrinsic apoptotic pathway and proposes that PMA is not overtly toxic at 10 nM concentration (particularly relative to staurosporine). It is also noteworthy that the results of the 4-hour resazurin-based assay may appear exaggerated. That is, the assay measures mitochondrial activity as a quantifier of cell viability; however, the intrinsic

**Fig. 3.** Proteins involved in the intrinsic apoptotic pathway. Proteins that were deactivated by PMA are indicated in green. Proteins that were activated by PMA are indicated in red. Proteins showing no statistically significant change are indicated in grey. Unevaluated proteins are indicated in white. Cytotoxicity was apparent after a 4 hour time period, but no long term impact on cell counts were observed after a 5 day time course.


https://doi.org/10.1016/j.heliyon.2018.e00617

apoptosis pathway requires increased mitochondrial permeability to facilitate the release of cytochrome c [42]. No statistical decrease in cell abundance was observed in the presence of PMA over a 5 day time course (Fig. 4B), suggesting that PMA is not inducing cell death. Thus, stimulation of the pathway may have a greater negative impact on mitochondrial function than on overall cell viability.

## 2.5. PMA regulation of cell proliferation

Several pathways that regulate cell growth and proliferation are activated in response to PMA (Table 3). Met, a tyrosine kinase receptor for hepatocyte growth factor (HGF), autophosphorylates upon HGF binding and promotes cell proliferation and motility [55]. Due to its role in cell survival, growth, and metastasis, Met has become a target for the develop of cancer therapeutics [56]. We observed a statistically significant increase of phosphorylated (activated) Met following 60 minutes of PMA exposure, indicating the potential for PMA induction of proliferation. Additionally, upregulation of phosphorylated polo-like kinase 1 (Plk1) was also observed after 60 minutes of PMA exposure. Plk1 acts as a DNA damage checkpoint in cell division and promotes mitosis upon phosphorylation at T210 [57]. An increase in phosphorylated Plk1 indicates increased cell division. Abl receptor tyrosine kinase, best known for the constitutively active Bcr-Abl fusion form implicated in chronic myelogenous leukemia, is significantly modified by PMA exposure [58]. Phosphorylation of Abl protein, as observed in our dataset, is activating, stimulating the receptor tyrosine kinase to promote cell proliferation [58].

However, not all PMA-induced effects on cell division pathways favored proliferation. An increase in Numb protein abundance, an inhibitor of Notch, was observed at 60 minutes. Numb promotes the ubiquitination and subsequent degradation of Notch [59] and prevents Notch from stimulating proliferation [60]. Interplay between tumor suppressor p53 and its inhibitor, MDM2, was also observed. Phosphorylation of MDM2, as observed in the data as a result of 60-minute PMA exposure, facilitates MDM2 ubiquitination of p53 and prevents p53 arrest of cell division. Thus, the increase in phosphorylated MDM2 favors proliferation. However, a greater abundance in p53 is also observed after 60-minute exposure to PMA, leaving question as to which effect was directly induced by PMA versus which likely resulted from negative feedback. Taken together, multiple proteins involved in regulating cell proliferation are modified by cellular exposure to PMA, but these signaling effects are likely competitive and may not yield an overall shift in favor of cell proliferation. As seen in Fig. 4B, the growth rate of 10 nM PMA treated T98G cells is identical to those treated with vehicle alone.

The reputation of PMA as both an apoptotic agent as well as a tumor promoter is contradictory. Generally, suppression of cell death/apoptosis is required for cell proliferation and tumor growth. Our protein signaling analysis revealed no definitive


https://doi.org/10.1016/j.heliyon.2018.e00617

shift in favor of apoptotic induction. Additionally, PMA appeared to concomitantly activate protein signaling pathways that promote cell proliferation equally as well as activating signaling pathways that suppress cell proliferation. Thus, at a PMA concentration that causes induction of NGF gene expression and secretion, PMA does not have a net effect on apoptosis or cell proliferation. Further, coadministration of 1 μM of the MEK inhibitor UO126 does not alter the effects of PMA on cell survival and growth. Hence, while higher concentrations of PMA may generate toxic properties well-attributed to the phorbol esters, these effects likely occur via mechanisms unrelated to the mechanisms by which PMA induces NGF.

## 2.6. PMA induction of NGF

As illustrated in Table 4 and Fig. 5, the MAPK pathway proteins Raf, MEK, and ERK show a statistically significant increase in phosphorylation following exposure to PMA. This pathway is of particular interest, as the transduction cascade is a

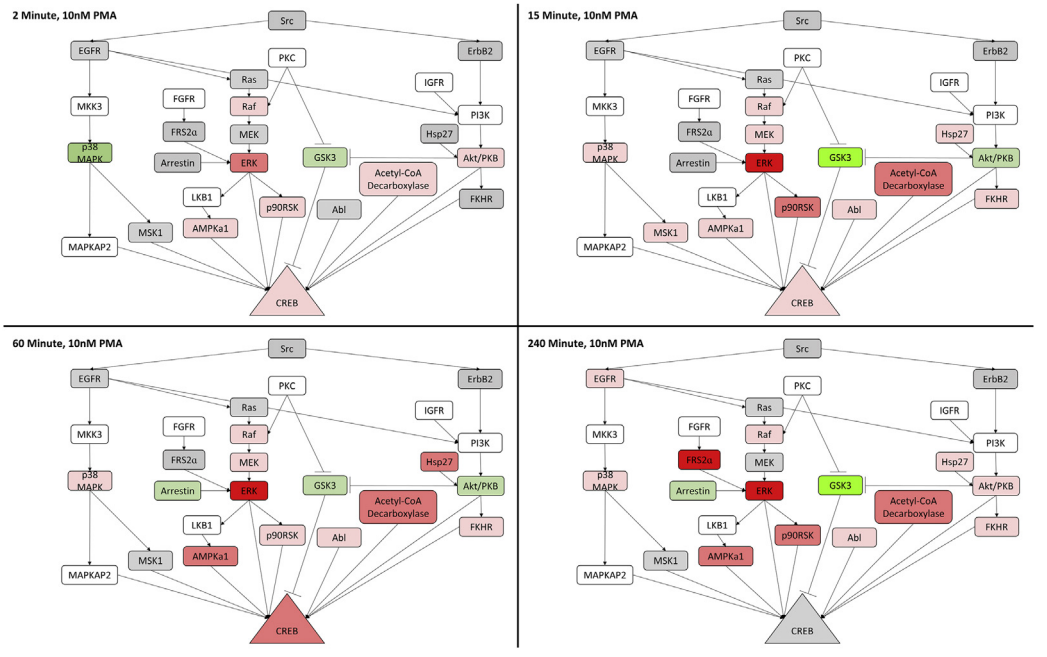


**Fig. 5.** A induced signal transduction. Cultured human glial cells were exposed to 10 nM PMA for the indicated durations and then the phosphorylation status of 135 select proteins (27 of which are shown in the figure) was assayed using RPPA. The red shading denotes an increase in activation state (measured by change in phosphorylation), the brightness of which is indicative of the magnitude of the change (light pink [20−99% increase over control] < dark pink [100%−199%] < red [200+%]). Proteins shaded green demonstrate a decrease in activation, relative to the vehicle treated cells, whereas proteins colored gray had no significant relative change (<20%). Proteins colored white were not assayed by RPPA but are included in the figure due to their established associations with the proteins that were assayed. The MAPK proteins Raf, MEK, and ERK become increasingly active as time progresses, culminating in maximum activation of CREB at 60 minutes. It is also noteworthy that, to varying degrees, multiple regulators of CREB outside of the MAPK pathway are also affected by PMA, including AMPKa1 (adenosine monophosphate kinase alpha-1), acetyl-CoA decarboxylase, FKHR (forkhead homolog in rhabdomyosarcoma), MSK1 (mitogen synthase kinase-1) and Akt/PKB (protein kinase B).


https://doi.org/10.1016/j.heliyon.2018.e00617

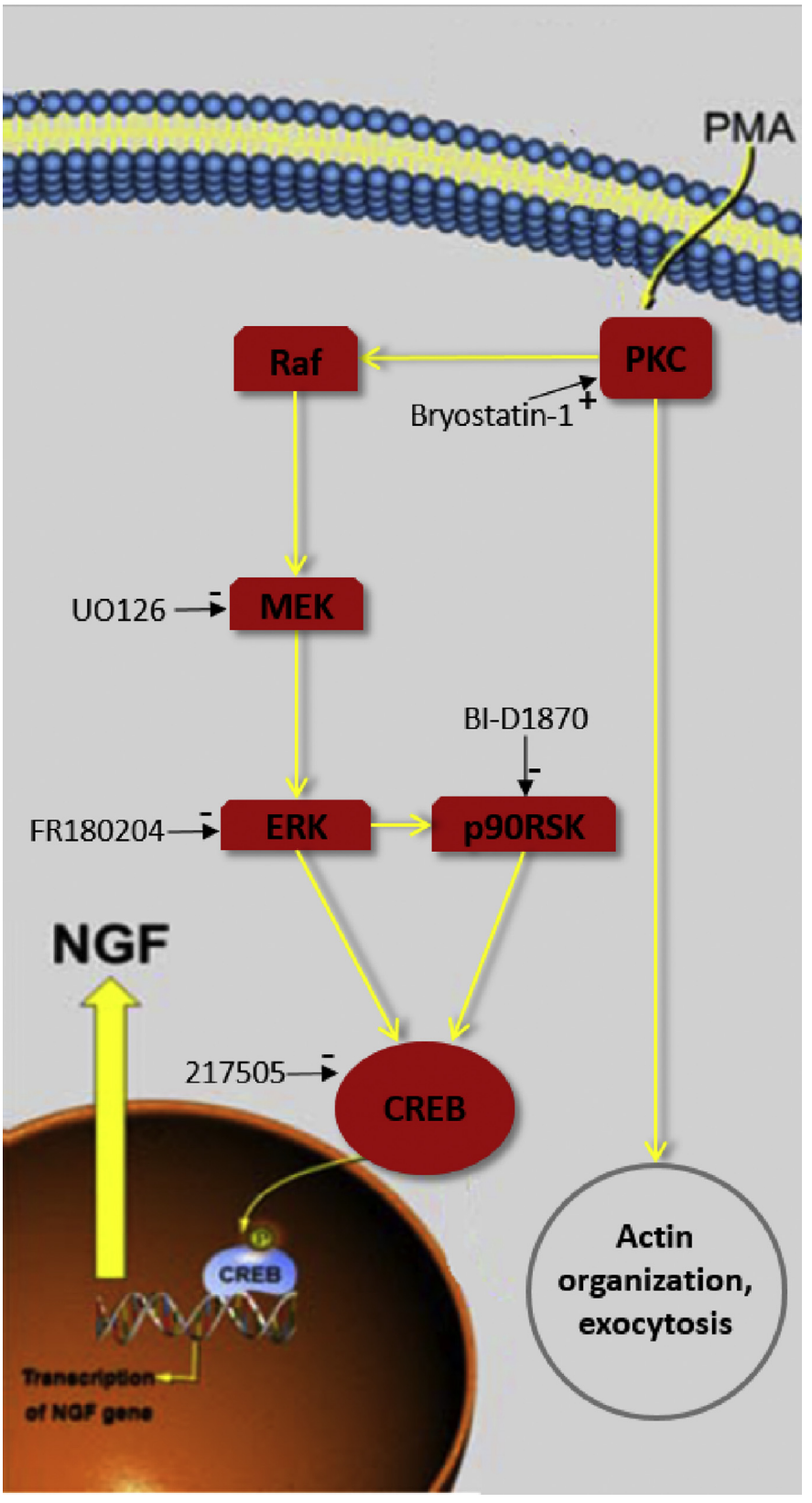



https://doi.org/10.1016/j.heliyon.2018.e00617

known target of PKC signaling and is capable of stimulating CREB activity. No significant change in phosphorylated Ras was observed, suggesting direct activation of Raf by PKC, a phenomenon previously described by others [61, 62]. A 270% increase in phosphorylated Raf is observed 60 minutes after exposure of the cells to PMA, whereas phosphorylated MEK increased by over 25% at 15 minutes and 60 minutes. An increased abundance of phosphorylated ERK was observed at all time points, ranging from a rise of 160% observed at 2 minutes ($p = 0.057$) to 370% observed at 15 minutes. The protein p90RSK was also activated by PMA throughout the time course (as was the RSK3 isoform; not shown in the figure), with significant increases in phosphorylated p90RSK observed between 2 minutes and 60 minutes, increasing in abundance by 60%−170%, respectively (phosphorylated RSK3 was 250% more abundant following 240 minute exposure to PMA). Phosphorylated CREB, a critical transcription factor for neurotrophin expression, exhibited a 200% increase after 60 minutes. Hence, the temporal signal transduction map generated from RPPA analysis highlighted PKC, Raf, MEK, ERK, p90RSK, and CREB as the key signal transduction proteins linking PMA with glial cell expression and secretion of NGF (Fig. 6).

## 2.7. Validating the involvement of the MAPK pathway

Our RPPA results indicated that upon PMA binding to and activating PKC, the signal transduction cascade proceeds through the MAPK proteins Raf, MEK, and ERK, leading to phosphorylation and activation of CREB. Concurrent activation of p90RSK, another CREB-acting kinase, may be required for maximal NGF induction. To validate the involvement of these proteins in NGF induction, we specifically targeted their activity using commercially available, cell permeable, selective agonists or antagonists (Fig. 6). In parallel, we also performed cell viability assays with each of the pathway modulators, to evaluate if cytotoxicity might contribute to the validation assay outcome.

As shown in Fig. 6 the macrocyclic lactone known as bryostatin-1 is a selective agonist of PKC. Cell viability assays performed with cultured human glial cells indicate that 10 nM bryostatin-1 does not have a detrimental effect on cell viability (Fig. 7A). Additionally, the NGF-specific ELISA reveals that at 10 nM concentration, bryostatin-1 may be a more potent inducer of NGF secretion by glial cells than is PMA (Fig. 7B), generating more NGF secretion at equivalent concentrations. Further, quantitative PCR indicates that 10 nM bryostatin-1 causes a four-fold

**Fig. 6.** The PMA signal transduction pathway leading to NGF induction. RPPA-based screening of the phosphorylation state of 135 signal transduction proteins highlighted Raf, MEK, ERK, p90RSK, and CREB as participants in a human glial cell signal transduction cascade activated by PMA binding to PKC. The agonists and antagonists chosen to validate the involvement of these proteins are indicated in the figure.


https://doi.org/10.1016/j.heliyon.2018.e00617

increase in NGF gene expression relative to cells treated with vehicle alone (Fig. 7C). Collectively, two structurally distinct PKC agonists induced NGF upregulation; thus validating the involvement of PKC in small molecule induction of NGF.

UO126, a MEK specific inhibitor (Fig. 6), demonstrates no significant detrimental effects on cell viability when cultured glial cells are treated with UO126 (Fig. 8A). PMA induction of glial cell NGF release was completely inhibited with 10 nM UO126 (Fig. 8B). Further, pre-treatment of glial cells with the MEK inhibitor successfully suppressed PMA induction of NGF gene expression in a dose-dependent manner (Fig. 8C).

Similarly, FR180204, a specific inhibitor of ERK (Fig. 6), demonstrated no detrimental effects on glial cell viability when the cells were treated with either FR180204 alone or with a combination of PMA and FR180204 (Fig. 9A). PMA induction of glial cell NGF secretion was significantly reduced with 10 nM FR180204 (Fig. 9B). Pre-treatment of the cells with FR180204 reduced PMA induction of NGF gene expression in a dose-dependent manner (Fig. 9C).

Our RPPA results suggested the involvement of p90RSK (and the RSK3 isoform) in the PMA signal transduction cascade. Following activation by ERK, both ERK and

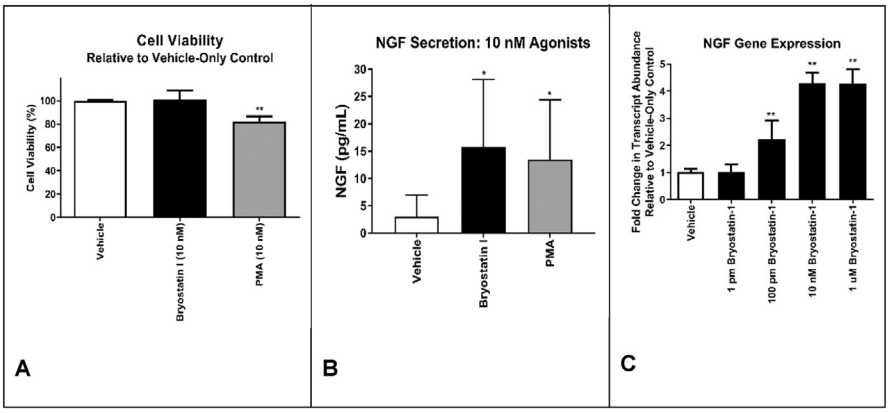


**Fig. 7.** Effects of bryostatin-1 on NGF gene expression and secretion. A) T98G cells were treated with Bryostatin (10 nM), PMA (10 nM) or vehicle alone for four hours. After four hours, cell viability was measured by resazurin assay. Percent viability is relative to the culture exposed to vehicle alone. While PMA demonstrates some measurable toxicity, bryostatin-1 has no detrimental effect on cell viability ($p > 0.05$, $n = 6$). Both PMA and bryostatin-1 were assayed at 10 nM concentration. B) Conditioned media obtained from human glial cell cultures exposed to either vehicle (DMSO), bryostatin-1, or PMA were assayed for NGF content using the NGF-specific ELISA. The PKC agonist bryostatin-1 induces NGF secretion from the cultured glial cells. NGF titers were determined after 4 hr. incubation, with both PMA and bryostatin-1 at 10 nM concentration. Both agonists demonstrated statistically significant induction of NGF secretion ($n = 6$). C) Quantitative PCR assessment of NGF transcript in human glial cell cultures treated with vehicle (DMSO) and increasing concentrations of bryostatin-1. Non-linear regression fitting a dose-response curve indicates the half-maximal activity of bryostatin-1 gene induction occurs at 170 pm ($R^2 = 0.91$). All graphs are expressed as Mean + SD.


https://doi.org/10.1016/j.heliyon.2018.e00617

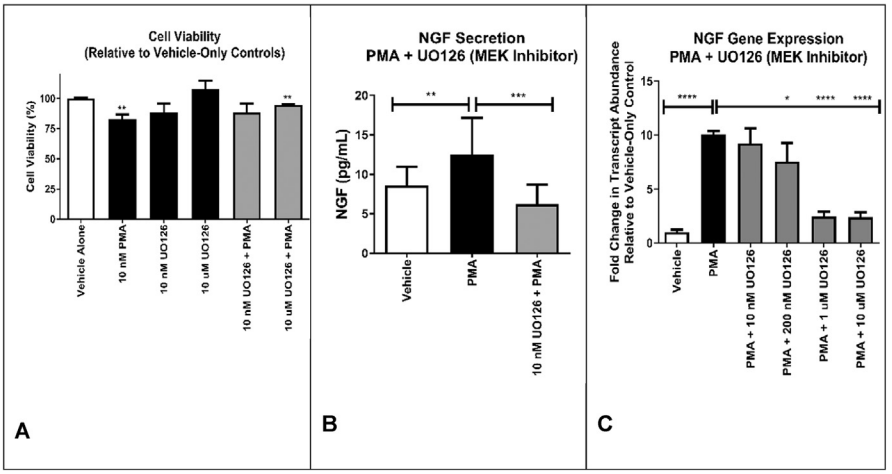


**Fig. 8.** Effects of the MEK inhibitor UO126 on PMA induction of NGF gene expression and secretion. A) A colorimetric assay with alamar blue was used to determine the viability of cultured glial cells exposed to vehicle (DMSO) or 10 nM PMA in conjunction with various concentrations of UO126, as indicated. Percent viability is relative to the culture exposed to vehicle. UO126 alone has little effect on glial cell viability (n = 6). B) Conditioned media obtained from human glial cell cultures exposed to either vehicle (DMSO), 10 nM PMA, or 10 nM PMA+10 nM UO126 were assayed for NGF content using the NGF-specific ELISA. The glial cells were preincubated with UO126 for 20 mins, then PMA was added and NGF titers were determined after a 4 hr incubation. UO126 eliminates PMA-induced glial cell NGF secretion (n = 6). C) Quantitative PCR assessment of NGF transcript in human glial cell cultures treated with vehicle (DMSO), 10 nM PMA, or 10 nM PMA coupled with various concentrations of UO126, as indicated. UO126 reduces PMA-induced NGF gene expression in a dose-dependent manner. Statistical significance (t-test PMA versus vehicle, PMA versus PMA + Inhibitor) indicated when applicable (n = 6). Non-linear regression fitting a dose-response curve indicates the half-maximal inhibitory activity of UO126 occurs at 401 nM ($R^2$ = .803). All graphs are expressed as Mean + SD.

p90RSK might then phosphorylate CREB, thereby initiating transcription of the NGF gene (see Fig. 6). BI-D1870, a specific inhibitor of p90RSK, demonstrates no deleterious effect on cultured glial cell viability (Fig. 10A). Further, the p90RSK inhibitor significantly reduced PMA induction of NGF release (Fig. 10B). However, BI-D1870 had no measurable effect on NGF gene expression (Fig. 10C). Hence, p90RSK appears to participate in the exocytosis of NGF, but not in regulation of NGF gene expression.

## 3. Conclusions

The reputation of PMA as both a tumor promoter and apoptotic agent is inherently counterintuitive, as tumor growth requires excessive cell survival and suppression of apoptotic pathways in proliferating cells. Our early time course results indicate that, when applied at low (therapeutically relevant) concentrations, PMA briefly induces a mild toxicity that alleviates shortly thereafter. Additionally, although we observed statistically significant changes in the abundance of active oncoproteins, supporting a role for PMA in tumorigenesis, PMA also activates signaling pathways involved in


https://doi.org/10.1016/j.heliyon.2018.e00617

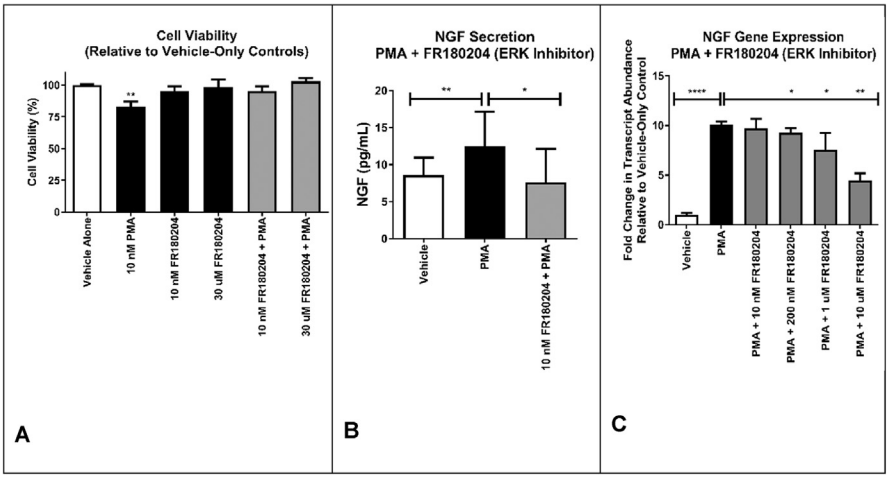


**Fig. 9.** Effects of the ERK inhibitor FR180204 on PMA induction of NGF gene expression and secretion. A) An alamar blue assay was used to determine the viability of cultured human glial cells exposed to vehicle (DMSO) or 10 nM PMA in conjunction with various concentrations of FR180204, as indicated. Percent viability is relative to the culture exposed to vehicle. FR180204 alone has no substantial effect on glial cell viability (n = 6). B) Conditioned media obtained from human glial cell cultures exposed to either vehicle (DMSO), 10 nM PMA, or 10 nM PMA+10 nM FR180204 were assayed for NGF content using the NGF-specific ELISA. The glial cells were preincubated with FR180204 for 20 mins, then PMA was added and NGF titers were determined after a 4 hr incubation. FR180204 reduces PMA-induced glial cell NGF secretion (n = 6). C) Quantitative PCR assessment of NGF transcript in human glial cell cultures treated with vehicle (DMSO), 10 nM PMA, or 10 nM PMA coupled with various concentrations of FR180204, as indicated. FR180204 reduces PMA-induced NGF gene expression in a dose-dependent manner. Statistical significance (t-test PMA versus vehicle, PMA versus PMA + Inhibitor) indicated when applicable (n = 6). Non-linear regression fitting a dose-response curve indicates the half-maximal inhibitory activity of FR180204 occurs at 1.90 uM ($R^2 = 0.828$). All graphs are expressed as Mean + SD.

suppressing cell proliferation. The cumulative effects of 10 nM PMA with respect to toxicity, apoptosis, and proliferation may offset, as no measurable change in T98G cell growth rate over a five day time course was observed in comparison to vehicle alone (Fig. 4.). While the MAPK/ERK pathway has been correlated to cancer development, many of the oncoproteins affected by PMA are unrelated to the MAPK cascade of proteins, suggesting that PMA induction of tumorigenesis observed at higher concentrations with chronic dosages is likely multifaceted and not linked to one central mechanism. Direct antagonism of the MAPK/ERK proteins had no effect on cell proliferation, while significantly affecting NGF gene expression.

NGF is known to have protective and regenerative effects against neurodegeneration and neuronal cell death [12, 17, 23, 36]. NGF upregulation involves gene expression coupled with protein translation, and/or exocytosis of NGF stored in vesicles within the glial cells. In addition to causing NGF secretion, an ideal therapeutic for neurodegenerative disease should replenish the NGF supply for constitutive release. Elucidation of glial cell signal transduction pathways leading to upregulation of NGF biosynthesis and secretion will facilitate the development of therapeutics that could


https://doi.org/10.1016/j.heliyon.2018.e00617

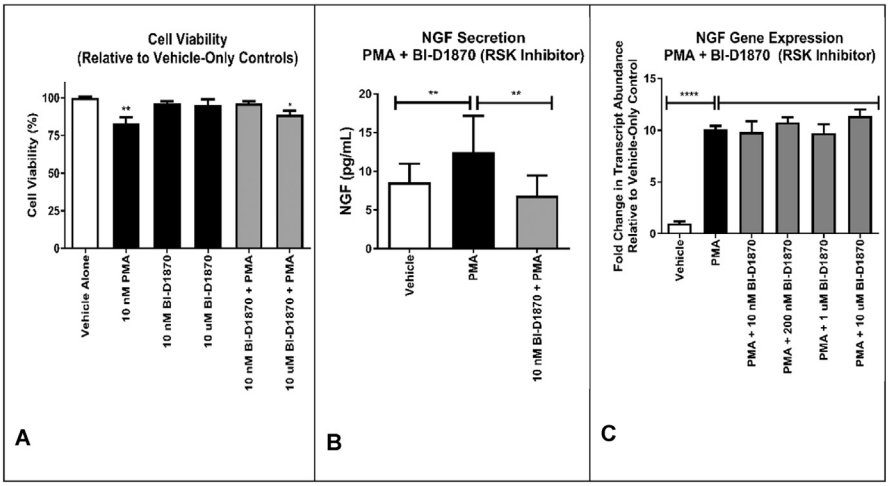


**Fig. 10.** Effects of the p90RSK Inhibitor BI-D1870 on PMA induction of NGF gene expression and secretion. A) An alamar blue colorimetric assay was used to determine the viability of cultured human glial cells exposed to vehicle (DMSO) or 10 nM PMA in conjunction with various concentrations of BI-D1870, as indicated. Percent viability is relative to the culture exposed to vehicle. BI-D1870 alone has no significant effect on glial cell viability (n = 6). B) Conditioned media obtained from human glial cell cultures exposed to either vehicle (DMSO), 10 nM PMA, or 10 nM PMA+10 nM BI-D1870 were assayed for NGF content using the NGF-specific ELISA. The glial cells were preincubated with BI-D1870 for 20 mins, then PMA was added and NGF titers were determined after a 4 hr incubation. BI-D1870 reduces PMA-induced glial cell NGF secretion (n = 6). C) Quantitative PCR assessment of NGF transcript in human glial cell cultures treated with vehicle (DMSO), 10 nM PMA, or 10 nM PMA coupled with various concentrations of BI-D1870, as indicated. Statistical significance (t-test PMA versus vehicle, PMA versus PMA + Inhibitor) indicated when applicable (n = 6). BI-D1870 has no significant effect on PMA induced NGF gene expression. All graphs are expressed as Mean + SD.

delay or reverse the effects of Alzheimer's disease or traumatic brain injury. Thus, a key aim of our investigation was to identify and validate signaling pathways underlying NGF induction.

Our reverse phase protein microarray and subsequent validation studies directly link PMA upregulation of NGF to cAMP Response Binding Element (CREB), a key transcription factor for neurotrophin expression (Fig. 11). Subsequent examination and validation confirmed the involvement and sequential activation of MEK, ERK, and finally CREB as the mechanism by which PMA induces NGF gene expression. Additionally, our investigation also highlighted p90RSK as an integral component of NGF secretion (Fig. 11). The identification of signaling pathways that stimulate NGF expression and secretion represents a critical step in identifying potential targets for the therapeutic treatment of neurodegeneration.

While PKC activators have begun to receive attention as potential cognition and memory enhancers [63, 64, 65, 66], challenges remain when designing PKC-specific therapeutics. For instance, the macrolide bryostatin-1 has been shown to cause significant adverse effects in preclinical and clinical trials as an anticancer therapeutic, including suppression of oxidative phosphorylation and induction of


https://doi.org/10.1016/j.heliyon.2018.e00617

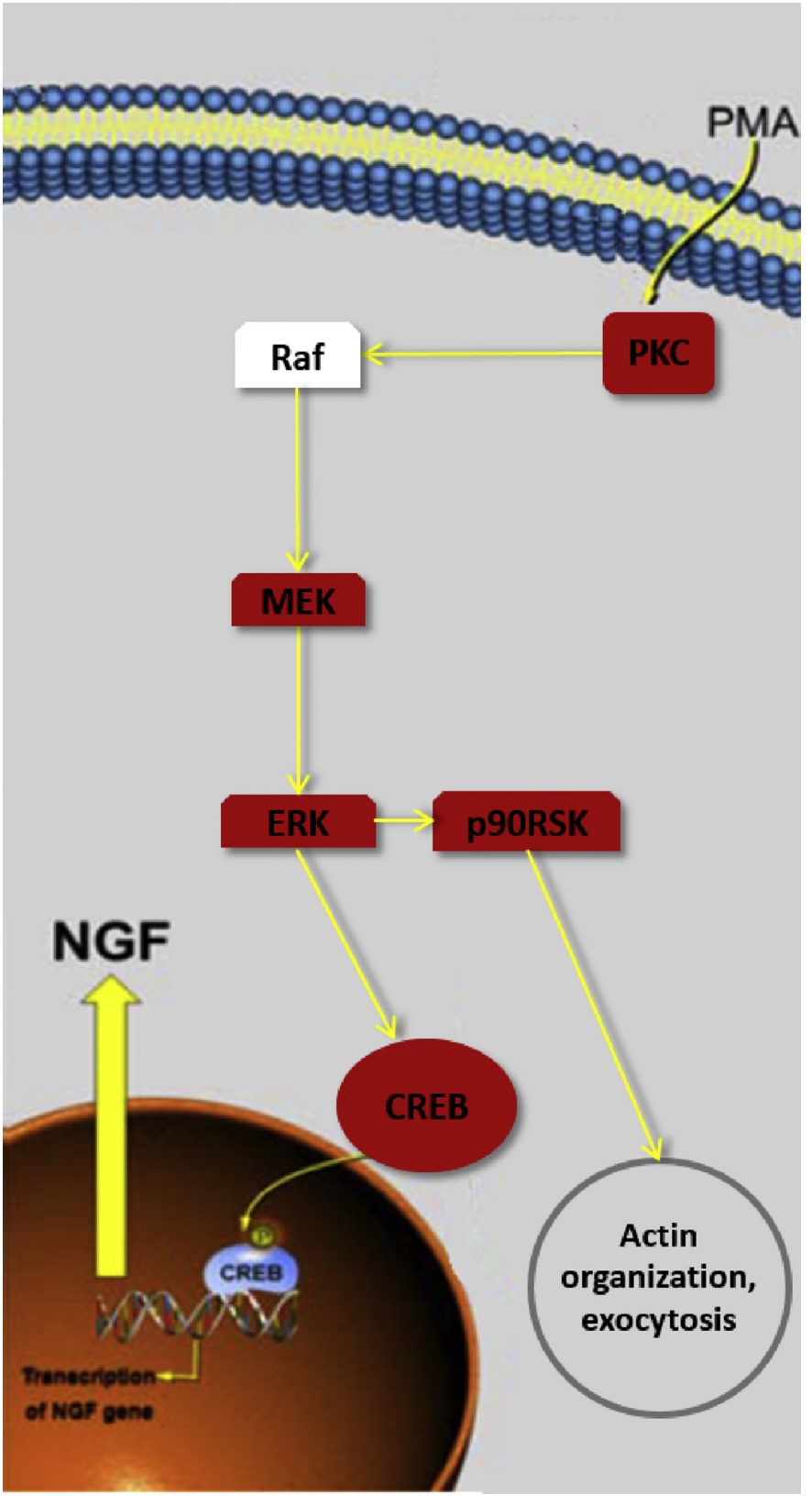



https://doi.org/10.1016/j.heliyon.2018.e00617

myalgia [67, 68]. However, in a phase II clinical trial for the treatment of Alzheimer's Disease, bryostatin-1 demonstrated no serious adverse effects and resulted in a marked improvement in cognitive function versus placebo [69]. The non-selective targeting of the many novel and conventional PKC isoforms, as well as their intracellular ubiquity, poses a challenge to the rational drug design of PKC activators as a therapy involving NGF upregulation. Targeting proteins that are downstream of PKC, but still essential to NGF upregulation, may be a more tractable approach to treating neurodegenerative disease.

Due to their relevance in oncology, therapeutic inhibitors (antagonists) of the MAPK signaling proteins have been sought and successfully developed [70, 71, 72]. For example, Trametinib, a clinically approved MEK antagonist for the treatment of myeloma, is a non-competitive inhibitor that binds to an allosteric site near the binding domain of ATP and prevents the association of ATP with the enzyme [73]. Further, clinically approved B-Raf inhibitors, vemurafenib and dabrafenib inhibit the mutated B-Raf$^{V600E}$ enzyme, preventing MEK activation in patients with the mutation [74]. However, these Raf inhibitors have also shown the ability to agonize the MAPK cascade when not supplemented with a MEK inhibitor, due to a phenomenon described as the Raf paradox [74], a mechanism by which wild-type Raf and mutated B-Raf activate by alternative mechanisms in response to small molecule inhibition [74, 75]. While direct small-molecule agonists of the MAPK proteins remain to be seen, the successful development of clinical approved selective MAPK pathway inhibitors highlights the overall druggability of these particular protein targets.

Although the results presented herein identify the PKC-MAPK-CREB axis as a central, critical element of PMA induction of NGF, it is noteworthy that additional proteins may also participate in the response. Our reverse phase microarray results show PMA-induced changes in the abundance of phosphorylated MSK1, GSK3alpha, p70S6kinase, SAPK/JNK, AMPKa1, and Elk1. It is notable that MSK1 (mitogen- and stress-activated protein kinase) is postulated to be involved in the upregulation of CREB [76, 77] and may serve as an alternative target for neuroprotection-related drug development.

In conclusion, we have identified and validated the PKC-MAPK-CREB pathway as integral to PMA/bryostatin 1 induction of NGF. These signal transduction proteins may all serve as targets for the rational development of NGF-promoting therapeutics. Efforts are now underway to develop these agonists and to assess the role of the additional transduction proteins found activated by exposure of the cell to PMA.

**Fig. 11.** The PMA signal transduction pathway leading to NGF upregulation. PMA stimulation of PKC leads to the activation of the MAPK signaling proteins Raf, MEK, and ERK. The MAPK proteins induce NGF expression via the signal transduction factor CREB. The protein p90RSK acts as a regulator of NGF secretion, but appears to play no role in NGF transcription. The involvement of proteins shaded red were all directly validated in this investigation.


https://doi.org/10.1016/j.heliyon.2018.e00617

# 4. Methods & materials

## 4.1. Cell culture

Human T98G glial cells (ATCC CRL-1690) were obtained from American Type Culture Collection (Manassas, VA, USA). T98G cells were cultured at 37 °C, 5% CO2 in 6 well plates containing Dulbecco's modified Eagle's medium (DMEM; Invitrogen, Carlsbad, CA, USA) containing 10% fetal bovine serum (FBS; Invitrogen).

## 4.2. ELISA

T98G cells were removed from tissue culture flasks using a trypsin−EDTA solution devoid of calcium and magnesium (Invitrogen) and plated to achieve confluent density into six-well plates containing DMEM w/10% FBS. 24 h before induction assays, the media was changed to OptiMEM I (reduced serum media; Invitrogen). To begin each cell assay, media was changed to OptiMEM I containing phorbol 12-myristate 13 acetate (PMA; Sigma-Aldrich, St. Louis, MO USA) with inhibitor or vehicle alone (DMSO). After assay completion, the conditioned media was harvested and NGF titers were determined using a Human b-NGF ELISA Development Kit (Peprotech, Rocky Hill, NJ USA) per the manufacturer's instructions. Purified recombinant human b-NGF (Peprotech) was used to create a standard curve ($A_{450}$ vs. NGF concentration).

## 4.3. qRT-PCR

Gene expression analysis was performed following mRNA extraction of whole cell lysates using RNEasy RNA isolation kits (Qiagen, Hilden, Germany). Reverse transcription was performed using random hexamers (Promega, Madison WI USA), dNTP (Invitrogen), and M-MLV reverse transcriptase (Promega). Real time PCR was performed on a Qiagen Rotor Gene Q using Rotor Gene Q master mix (Qiagen) according to manufacturer's protocol. PCR primers (Sigma Aldrich) for NGF were F: 5′-CCAATAACAGTTTTACCAAGGGAGCAGC-3′, R: 5′-CAAGGGAATGCTGAAGTTTAGTCCAGTG-3′. TATA box binding (TBP) protein was used as a reference gene. Primers for TBP were F: 5′-CCACAGTGAATCTTGGTTGTAAACTTGACC-3′ and R: 5′-GTGGTTCGTGGCTCTCTTATCCTC-3′.

## 4.4. Reverse phase protein microarrays

Approximately 9 nl of each cell lysate was printed onto nitrocellulose-coated slides (Grace BioLabs, Bend, OR, USA) in triplicate using a 2470 Aushon Arrayer (Aushon BioSysterms, Billerca, MA, USA). Samples were printed along with a series of standard curves of positive and negative control lysates for quality assurance.


https://doi.org/10.1016/j.heliyon.2018.e00617

For estimation of total protein amounts, selected arrays were stained with Sypro Ruby Protein Blot Stain (Invitrogen, Carlsbad, CA) according to the manufacturer's instructions and visualized on a Powerscanner fluorescent scanner (Tecan US, Inc., Research Triangle Park, NC). To prepare printed slides for staining, Reblot (Cehmicaon, Temecula, CA) was applied for 15 minutes and followed by two successive washes with PBS for 5 minutes each. Slides were then placed in 1 g I-block blocking solution (Applied Biosystems, Bedford, MA) prepared with 0.5% Tween-20 in 500 mL PBS. Blocking took place under constant rocking for at least one hour.

An automatic slide stainer (DakoCytomation, Carpinteria, CA) was used to stain the blocked arrays with antibodies using the Catalyzed Signal Amplification System kit (CSA; Dako). Per the manufacturer's recommendation, the biotin blocking kit (DAKO) is used to block endogenous biotin for 10 minutes. A protein block is then introduced for 5 minutes. Primary antibodies are diluted in the provided antibody diluent and incubated on slides for 30 minutes. A biotinylated secondary antibody then follows for 15 minutes. A streptavidin-biotin-peroxidase complex is used for signal amplification and applied for 15 minutes, with the amplification reagent (biotinyl-tyramide/hydrogen peroxide, streptavidin-peroxidase) applied for 15 minutes each. Steptavidin-conjugated IRDye680 (LI-COR, Lincoln, NE) is used to generate signal. Slides were allowed to air dry following development.

Western blotting of cell lysate controls (e.g. Hela +/− pervandate, Jurkat +/− Calyculin) was used to validate each antibody for the presence of a single band of appropriate MW and phosphorylation specificity.

## 4.5. Statistical analysis

Six-replicate reverse phase microarray data from treated and untreated cells were compared using a two-tailed unpaired heteroscedastic t-test. Comparisons generating p-values $< 0.05$ were considered significant. For statistically significant analytes, $\log_2$ fold change was determined using the median values for the individual treated and untreated data sets. Two-tailed unpaired heteroscedastic t-tests were also used to evaluate statistical significance for NGF secretion, NGF gene expression, and cytotoxicity assays (described below). All figures are plotted with error bars as Mean + SD. P-values are indicated as $p \leq 0.05$ labeled with one asterisk, $p \leq 0.01$ labeled with two asterisks, $p \leq 0.001$ labeled with 3 asterisks, and $p \leq 0.0001$ labeled with 4 asterisks. P values greater than 0.05 are unlabeled or labeled as *ns* for clarity.

## 4.6. Cytotoxicity assays

After exposure to compound or vehicle-alone in OptiMEM I media for four hours, Alamar blue dye (ThermoFisher Scientific, Waltham, MA) was added directly to the media and allowed to incubate for one hour. Following incubation, $A_{570}/A_{600}$


https://doi.org/10.1016/j.heliyon.2018.e00617

measurements were made to calculate reduction of resazurin dye to resorufin. A ratio of reduction in treated versus untreated cells was calculated in order to determine overall cell viability.

## 4.7. Antagonist assays

Antagonist assays were performed using a 20 minute preincubation of cells with OptiMEM containing the inhibitor. UO126 (Sigma Aldrich), FR180204 (Merck Millipore, Billerica MA USA), BI-D1870 (Santa Cruz Biotechnology, Dallas, TX USA), 217505 (Merck Millipore) were solvated to equal concentrations in DMSO. Literature *in vitro* $IC_{50}$ values for intended targets were available as 10−30 nM for BI-D1870 [78] and 72 nM for UO126 [79]. Literature *in vivo* $IC_{50}$ values for intended targets were available as 2.9 uM for 217505 [80] and FR180204 [81]. In expectation that *in vitro* $IC_{50}$ values would be lower than *in vivo*, a range of concentrations was selected from below the predicted $IC_{50}$ value to above the predicted $IC_{50}$ value to show dose response as well as complete inhibition. The inhibitor 217505 was poorly soluble above 1 uM under our assay conditions. A complete dose response for 217505 was not performed, as the effects of CREB on NGF gene expression are already well documented and the highest usable dose had no effect on NGF secretion. NGF secretion experiments with UO126, FR180204, and BI-D1870 were always performed in tandem. To facilitate comparisons, NGF secretion experiments with 217505 were vehicle normalized to the other antagonist experiments.

# Declarations

## Author contribution statement

Justin B. Davis: Conceived and designed the experiments; Performed the experiments; Analyzed and interpreted the data; Wrote the paper.

Valerie Calvert: Performed the experiments; Analyzed and interpreted the data.

Steven Roberts, Sabrina Bracero: Performed the experiments.

Emanuel Petricoin: Conceived and designed the experiments; Analyzed and interpreted the data; Contributed reagents, materials, analysis tools or data.

Robin Couch: Conceived and designed the experiments; Analyzed and interpreted the data; Contributed reagents, materials, analysis tools or data; Wrote the paper.

## Funding statement

This work was supported by the Commonwealth Health Research Board (grant #247-01-12) and the Alzheimer's & Related Diseases Research Award Fund (Virginia Center on Aging grant #15-7).


https://doi.org/10.1016/j.heliyon.2018.e00617

## Competing interest statement

The authors declare no conflict of interest.

## Additional information

No additional information is available for this paper.

## Acknowledgements

Special thanks to Virginia Espina for critical discussion of the RPPA data. Data and materials availability: Data is available upon request.

## References

[1] M. Prince, A. Wimo, M. Guerchet, G.-C. Ali, Y.-T. Wu, M. Prina, World Alzheimer Report 2015: the Global Impact of Dementia: an Analysis of Prevalence, Incidence, Cost and Trends, August 2015.

[2] J. Davis, R. Couch, Strategizing the development of Alzheimer's therapeutics, Adv. Alzheimer's Dis. 03 (03) (2014) 107−127.

[3] E. Karran, M. Mercken, B.D. Strooper, The amyloid cascade hypothesis for Alzheimer's disease: an appraisal for the development of therapeutics, Nat. Rev. Drug Discov. 10 (9) (2011) 698−712.

[4] R.J. Castellani, M.A. Smith, Compounding artefacts with uncertainty, and an amyloid cascade hypothesis that is "too big to fail.", J. Pathol. 224 (2) (2011) 147−152.

[5] C. Ballatore, V.M.-Y. Lee, J.Q. Trojanowski, Tau-mediated neurodegeneration in Alzheimer's disease and related disorders, Nat. Rev. Neurosci. 8 (9) (2007) 663−672.

[6] D.M. Barten, P. Fanara, C. Andorfer, et al., Hyperdynamic microtubules, cognitive deficits, and pathology are improved in tau transgenic mice with low doses of the microtubule-stabilizing agent BMS-241027, J. Neurosci. Off. J. Soc. Neurosci. 32 (21) (2012) 7137−7145.

[7] R. Donev, M. Kolev, B. Millet, J. Thome, Neuronal death in Alzheimer's disease and therapeutic opportunities, J. Cell Mol. Med. 13 (11−12) (2009) 4329−4348.

[8] P.T. Francis, A.M. Palmer, M. Snape, G.K. Wilcock, The cholinergic hypothesis of Alzheimer's disease: a review of progress, J. Neurol. Neurosurg. Psychiatry 66 (2) (1999) 137−147.


https://doi.org/10.1016/j.heliyon.2018.e00617

[9] R. Schliebs, Basal forebrain cholinergic dysfunction in Alzheimer's disease—interrelationship with beta-amyloid, inflammation and neurotrophin signaling, Neurochem. Res. 30 (6-7) (2005) 895—908.

[10] M.H. Tuszynski, U.H. Sang, K. Yoshida, F.H. Gage, Recombinant human nerve growth factor infusions prevent cholinergic neuronal degeneration in the adult primate brain, Ann. Neurol. 30 (5) (1991) 625—636.

[11] M.H. Tuszynski, L. Thal, M. Pay, et al., A phase 1 clinical trial of nerve growth factor gene therapy for Alzheimer disease, Nat. Med. 11 (5) (2005) 551—555.

[12] M.S. Rafii, T.L. Baumann, R.A.E. Bakay, et al., A phase 1 study of stereotactic gene delivery of AAV2-NGF for Alzheimer's disease, Alzheimers Dementia J. Alzheimers. Assoc. (January 2014).

[13] E. Giacobini, G. Gold, Alzheimer disease therapy—moving from amyloid-β to tau, Nat. Rev. Neurol. 9 (12) (2013) 677—686.

[14] S.E. Counts, E.J. Mufson, The role of nerve growth factor receptors in cholinergic basal forebrain degeneration in prodromal Alzheimer disease, J. Neuropathol. Exp. Neurol. 64 (4) (2005) 263—272.

[15] C. Belka, W. Budach, Anti-apoptotic Bcl-2 proteins: structure, function and relevance for radiation biology, Int. J. Radiat. Biol. 78 (8) (2002) 643—658.

[16] J. Qian, Y. Zou, J.S.M. Rahman, B. Lu, P.P. Massion, Synergy between phosphatidylinositol 3-kinase/Akt pathway and Bcl-xL in the control of apoptosis in adenocarcinoma cells of the lung, Mol. Cancer Ther. 8 (1) (2009) 101—109.

[17] C. Yang, Y. Liu, X. Ni, N. Li, B. Zhang, X. Fang, Enhancement of the non-amyloidogenic pathway by exogenous NGF in an Alzheimer transgenic mouse model, Neuropeptides 48 (4) (2014) 233—238.

[18] A.S. Algarni, A.J. Hargreaves, J.M. Dickenson, Activation of transglutaminase 2 by nerve growth factor in differentiating neuroblastoma cells: a role in cell survival and neurite outgrowth, Eur. J. Pharmacol. 820 (2018) 113—129.

[19] S.D. Skaper, Neurotrophic factors: an overview, in: S.D. Skaper (Ed.), Neurotrophic Factors, vol. 1727, Springer New York, New York, NY, 2018, pp. 1—17.

[20] P.M. Friden, L.R. Walus, P. Watson, et al., Blood-brain barrier penetration and in vivo activity of an NGF conjugate, Science 259 (5093) (1993) 373—377.

[21] E. Dixon, T. Schweibenz, A. Hight, et al., Bacteria-induced static batch fungal fermentation of the diterpenoid cyathin A3, a small-molecule inducer of nerve growth factor, J. Ind. Microbiol. Biotechnol. 38 (5) (2010) 607—615.


https://doi.org/10.1016/j.heliyon.2018.e00617

[22] J.H. Kordower, V. Charles, R. Bayer, et al., Intravenous administration of a transferrin receptor antibody-nerve growth factor conjugate prevents the degeneration of cholinergic striatal neurons in a model of Huntington disease, Proc. Natl. Acad. Sci. U. S. A. 91 (19) (1994) 9077−9080.

[23] M.B. Rosenberg, T. Friedmann, R.C. Robertson, et al., Grafting genetically modified cells to the damaged brain: restorative effects of NGF expression, Science 242 (4885) (1988) 1575−1578.

[24] J. Barnett, P. Baecker, C. Routledge-Ward, et al., Human beta nerve growth factor obtained from a baculovirus expression system has potent in vitro and in vivo neurotrophic activity, Exp. Neurol. 110 (1) (1990) 11−24.

[25] M. Mosior, A.C. Newton, Mechanism of interaction of protein kinase C with phorbol esters. Reversibility and nature of membrane association, J. Biol. Chem. 270 (43) (1995) 25526−25533.

[26] Y.P. Hwang, H.J. Yun, J.H. Choi, K.W. Kang, H.G. Jeong, Suppression of phorbol-12-myristate-13-acetate-induced tumor cell invasion by bergamottin via the inhibition of protein kinase Cdelta/p38 mitogen-activated protein kinase and JNK/nuclear factor-kappaB-dependent matrix metalloproteinase-9 expression, Mol. Nutr. Food Res. 54 (7) (2010) 977−990.

[27] M.S. Rabin, P.J. Doherty, M.M. Gottesman, The tumor promoter phorbol 12-myristate 13-acetate induces a program of altered gene expression similar to that induced by platelet-derived growth factor and transforming oncogenes, Proc. Natl. Acad. Sci. U. S. A. 83 (2) (1986) 357−360.

[28] M.-T. Wang, M. Holderfield, J. Galeas, et al., K-Ras promotes tumorigenicity through suppression of non-canonical Wnt signaling, Cell 163 (5) (2015) 1237−1251.

[29] G. Goel, H.P.S. Makkar, G. Francis, K. Becker, Phorbol esters: structure, biological activity, and toxicity in animals, Int. J. Toxicol. 26 (4) (2007) 279−288.

[30] M.A. Hahn, G.C. Mayne, Phorbol ester-induced cell death in PC-12 cells overexpressing Bcl-2 is dependent on the time at which cells are treated, Cell Biol. Int. 28 (5) (2004) 345−359.

[31] C.A. Hall-Jackson, T. Jones, N.G. Eccles, et al., Induction of cell death by stimulation of protein kinase C in human epithelial cells expressing a mutant ras oncogene: a potential therapeutic target, Br. J. Cancer 78 (5) (1998) 641−651.

[32] J. Hrubik, B. Glisic, D. Samardzija, et al., Effect of PMA-induced protein kinase C activation on development and apoptosis in early zebrafish embryos, Comp. Biochem. Physiol. Toxicol. Pharmacol. CBP 190 (2016) 24−31.


https://doi.org/10.1016/j.heliyon.2018.e00617

[33] J.-F. Wang, S.-H. Yang, Y.-Q. Liu, et al., Five new phorbol esters with cytotoxic and selective anti-inflammatory activities from Croton tiglium, Bioorg. Med. Chem. Lett 25 (9) (2015) 1986−1989.

[34] J. Zheng, C. Kong, X. Yang, X. Cui, X. Lin, Z. Zhang, Protein kinase C-α (PKCα) modulates cell apoptosis by stimulating nuclear translocation of NF-kappa-B p65 in urothelial cell carcinoma of the bladder, BMC Cancer 17 (1) (2017) 432.

[35] H.-C. Cheng, Essential role of cAMP-response element-binding protein activation by A2A adenosine receptors in rescuing the nerve growth factor-induced neurite outgrowth impaired by blockage of the MAPK cascade, J. Biol. Chem. 277 (37) (2002) 33930−33942.

[36] A. Riccio, Mediation by a CREB family transcription factor of NGF-dependent survival of sympathetic neurons, Science 286 (5448) (1999) 2358−2361.

[37] A. Silvestri, V. Calvert, C. Belluco, et al., Protein pathway activation mapping of colorectal metastatic progression reveals metastasis-specific network alterations, Clin. Exp. Metastasis 30 (3) (2013) 309−316.

[38] V. Espina, J.D. Wulfkuhle, V.S. Calvert, E.F. Petricoin, L.A. Liotta, Reverse phase protein microarrays for monitoring biological responses, in: P.B. Fisher (Ed.), Cancer Genomics and Proteomics, Humana Press, Totowa, NJ, 2007, pp. 321−336.

[39] E.F. Petricoin, Mapping molecular networks using proteomics: a vision for patient-tailored combination therapy, J. Clin. Oncol. 23 (15) (2005) 3614−3621.

[40] S. Elmore, Apoptosis: a review of programmed cell death, Toxicol. Pathol. 35 (4) (2007) 495−516.

[41] Y. Tan, M.R. Demeter, H. Ruan, M.J. Comb, BAD Ser-155 phosphorylation regulates BAD/Bcl-XL interaction and cell survival, J. Biol. Chem. 275 (33) (2000) 25865−25869.

[42] D.M. Finucane, E. Bossy-Wetzel, N.J. Waterhouse, T.G. Cotter, D.R. Green, Bax-induced caspase activation and apoptosis via cytochromec release from mitochondria is inhibitable by Bcl-xL, J. Biol. Chem. 274 (4) (1999) 2225−2233.

[43] D. Westphal, G. Dewson, P.E. Czabotar, R.M. Kluck, Molecular biology of Bax and Bak activation and action, Biochim. Biophys. Acta BBA − Mol. Cell Res. 1813 (4) (2011) 521−531.


https://doi.org/10.1016/j.heliyon.2018.e00617

[44] H. Zou, Y. Li, X. Liu, X. Wang, An APAF-1.cytochrome c multimeric complex is a functional apoptosome that activates procaspase-9, J. Biol. Chem. 274 (17) (1999) 11549−11556.

[45] L.A. Allan, P.R. Clarke, Apoptosis and autophagy: regulation of caspase-9 by phosphorylation: regulation of caspase-9 by phosphorylation, FEBS J. 276 (21) (2009) 6063−6073.

[46] X. Fang, S. Yu, A. Eder, et al., Regulation of BAD phosphorylation at serine 112 by the Ras-mitogen-activated protein kinase pathway, Oncogene 18 (48) (1999) 6635−6640.

[47] J. Downward, How BAD phosphorylation is good for survival, Nat. Cell Biol. 1 (2) (1999) E33−E35.

[48] S. Takayama, J.C. Reed, S. Homma, Heat-shock proteins as regulators of apoptosis, Oncogene 22 (56) (2003) 9041−9047.

[49] A. Vidyasagar, N.A. Wilson, A. Djamali, Heat shock protein 27 (HSP27): biomarker of disease and therapeutic target, Fibrogenesis Tissue Repair 5 (1) (2012) 7.

[50] R.B. Nahomi, A. Palmer, K.M. Green, P.E. Fort, R.H. Nagaraj, Pro-inflammatory cytokines downregulate Hsp27 and cause apoptosis of human retinal capillary endothelial cells, Biochim. Biophys. Acta BBA − Mol. Basis Dis. 1842 (2) (2014) 164−174.

[51] C. Cohen, C.M. Lohmann, G. Cotsonis, D. Lawson, R. Santoianni, Survivin expression in ovarian carcinoma: correlation with apoptotic markers and prognosis, Mod. Pathol. Off. J. U. S. Can. Acad. Pathol. Inc. 16 (6) (2003) 574−583.

[52] K.K. Wang, Calpain and caspase: can you tell the difference? Trends Neurosci. 23 (1) (2000) 20−26.

[53] G. Chaitanya, J.S. Alexander, P. Babu, PARP-1 cleavage fragments: signatures of cell-death proteases in neurodegeneration, Cell Commun. Signal. 8 (1) (2010) 31.

[54] K.K. Lee, T. Ohyama, N. Yajima, S. Tsubuki, S. Yonehara, MST, a physiological caspase substrate, highly sensitizes apoptosis both upstream and downstream of caspase activation, J. Biol. Chem. 276 (22) (2001) 19276−19285.

[55] S.L. Organ, M.-S. Tsao, An overview of the c-MET signaling pathway, de Bono JS, ed. Ther. Adv. Med. Oncol. 3 (1_suppl) (2011) S7−S19.

[56] E. Gherardi, W. Birchmeier, C. Birchmeier, G.V. Woude, Targeting MET in cancer: rationale and progress, Nat. Rev. Cancer 12 (2) (2012) 89−103.


https://doi.org/10.1016/j.heliyon.2018.e00617

[57] L. Tsvetkov, D.F. Stern, Phosphorylation of Plk1 at S137 and T210 is inhibited in response to DNA damage, Cell Cycle Georget Tex 4 (1) (2005) 166−171.

[58] O. Hantschel, G. Superti-Furga, Regulation of the c-Abl and Bcr−Abl tyrosine kinases, Nat. Rev. Mol. Cell Biol. 5 (1) (2004) 33−44.

[59] M.A. McGill, C.J. McGlade, Mammalian numb proteins promote Notch1 Receptor ubiquitination and degradation of the Notch1 intracellular domain, J. Biol. Chem. 278 (25) (2003) 23196−23203.

[60] P. Rizzo, C. Osipo, K. Foreman, T. Golde, B. Osborne, L. Miele, Rational targeting of Notch signaling in cancer, Oncogene 27 (38) (2008) 5124−5131.

[61] W. Kolch, G. Heidecker, G. Kochs, et al., Protein kinase C alpha activates RAF-1 by direct phosphorylation, Nature 364 (6434) (1993) 249−252.

[62] S.-i. Hirai, Protein kinase C delta activates the MEK-ERK pathway in a manner independent of Ras and dependent on Raf, J. Biol. Chem. 271 (38) (1996) 23512−23519.

[63] M.-K. Sun, D.L. Alkon, Protein kinase C activators as synaptogenic and memory therapeutics, Arch. Pharm. (Weinheim) 342 (12) (2009) 689−698.

[64] M.-K. Sun, D.L. Alkon, Pharmacology of protein kinase C activators: cognition-enhancing and antidementic therapeutics, Pharmacol. Ther. 127 (1) (2010) 66−77.

[65] R. Etcheberrigaray, M. Tan, I. Dewachter, et al., Therapeutic effects of PKC activators in Alzheimer's disease transgenic mice, Proc. Natl. Acad. Sci. 101 (30) (2004) 11141−11146.

[66] T.K. Khan, T.J. Nelson, V.A. Verma, P.A. Wender, D.L. Alkon, A cellular model of Alzheimer's disease therapeutic efficacy: PKC activation reverses Aβ-induced biomarker abnormality on cultured fibroblasts, Neurobiol. Dis. 34 (2) (2009) 332−339.

[67] P.F. Hickman, G.J. Kemp, C.H. Thompson, et al., Bryostatin 1, a novel antineoplastic agent and protein kinase C activator, induces human myalgia and muscle metabolic defects: a 31P magnetic resonance spectroscopic study, Br. J. Cancer 72 (4) (1995) 998−1003.

[68] D. Mochly-Rosen, K. Das, K.V. Grimes, Protein kinase C, an elusive therapeutic target? Nat. Rev. Drug Discov. 11 (12) (2012) 937−957.

[69] T.J. Nelson, M.-K. Sun, C. Lim, et al., Bryostatin effects on cognitive function and PKCε in Alzheimer's disease phase IIa and Expanded access trials, J. Alzheimers Dis. 58 (2) (2017) 521−535.

 https://doi.org/10.1016/j.heliyon.2018.e00617

[70] P.J. Roberts, C.J. Der, Targeting the Raf-MEK-ERK mitogen-activated protein kinase cascade for the treatment of cancer, Oncogene 26 (22) (2007) 3291−3310.

[71] D. Wang, S.A. Boerner, J.D. Winkler, P.M. LoRusso, Clinical experience of MEK inhibitors in cancer therapy, Biochim. Biophys. Acta BBA − Mol. Cell Res. 1773 (8) (2007) 1248−1255.

[72] L. Santarpia, S.M. Lippman, A.K. El-Naggar, Targeting the MAPK-RAS-RAF signaling pathway in cancer therapy, Expert Opin. Ther. Targets 16 (1) (2012) 103−119.

[73] J.J. Luke, P.A. Ott, New developments in the treatment of metastatic melanoma − role of dabrafenib-trametinib combination therapy, Drug Healthc. Patient Saf. 6 (2014) 77−88.

[74] M. Holderfield, T.E. Nagel, D.D. Stuart, Mechanism and consequences of RAF kinase activation by small-molecule inhibitors, Br. J. Cancer 111 (4) (2014) 640−645.

[75] C.A. Hall-Jackson, P.A. Eyers, P. Cohen, et al., Paradoxical activation of Raf by a novel Raf inhibitor, Chem. Biol. 6 (8) (1999) 559−568.

[76] J.S. Arthur, P. Cohen, MSK1 is required for CREB phosphorylation in response to mitogens in mouse embryonic stem cells, FEBS Lett. 482 (1-2) (2000) 44−48.

[77] G.R. Wiggin, A. Soloaga, J.M. Foster, V. Murray-Tait, P. Cohen, J.S.C. Arthur, MSK1 and MSK2 are required for the mitogen- and stress-induced phosphorylation of CREB and ATF1 in fibroblasts, Mol. Cell Biol. 22 (8) (2002) 2871−2881.

[78] G.P. Sapkota, L. Cummings, F.S. Newell, et al., BI-D1870 is a specific inhibitor of the p90 RSK (ribosomal S6 kinase) isoforms in vitro and in vivo, Biochem. J. 401 (1) (2007) 29.

[79] M.F. Favata, K.Y. Horiuchi, E.J. Manos, et al., Identification of a novel inhibitor of mitogen-activated protein kinase kinase, J. Biol. Chem. 273 (29) (1998) 18623−18632.

[80] B.X. Li, X. Xiao, Discovery of a small-molecule inhibitor of the KIX-KID interaction, Chembiochem. Eur. J. Chem. Biol. 10 (17) (2009) 2721−2724.

[81] M. Ohori, T. Kinoshita, M. Okubo, et al., Identification of a selective ERK inhibitor and structural determination of the inhibitor−ERK2 complex, Biochem. Biophys. Res. Commun. 336 (1) (2005) 357−363.


https://doi.org/10.1016/j.heliyon.2018.e00617